A post-processing method for 3D fundus image enhancement

Andrey Krylov, Andrey Nasonov, Alexander Razgulin, Tatiana Romanenko
Laboratory of Mathematical Methods of Image Processing
Faculty of Computational Mathematics and Cybernetics
Lomonosov Moscow State University
119991, Russia, Moscow, Leninskie Gory, MGU BMK
Email: kryl@cs.msu.ru

***Abstract*—A method of enhancing the 3D structure of fundus images has been developed. It is based on grid warping techniques and ensures both denoising and vessel sharpening of fundus images. The method has been tested with phantom translucent 3D object of vessels processed using Tikhonov regularization method.**

Keywords: 3D image sharpening, fundus images, image denoising

I. Introduction

One of the main problems arising in ophthalmology is non-invasive restoration of the 3D structure of human eye fundus for a consequent diagnosis of diseases. Recently, a promising adaptive optics approach was suggested in [1] to restore 3D structure of human fundus "in vivo". It is based on the rapid refocusing of imaging system. By properly varying the focal length one can obtain a stack of images, each corresponding to different depths of cross section. Having a sufficient amount of sections, one can try to reconstruct the original 3D object by known methods. Unfortunately, in most cases the result will not be satisfactory. The fact is that images, captured in each focal plane, contain true cross sections of the 3D object and, moreover, defocused images of neighboring sections of the depth, aberrations of eye optical system, fixation fluctuations, distortions of light-sensitive sensors, etc. Thus, the problem is to elaborate robust approach capable of obtaining a stack of cross section images which are purified from such distortions. Note that analogous approach in bio-microscopy is also known as digital sectioning [2]–[4].

In this paper, we use the 3D object restoration process and propose an image enhancement post-processing method. It is based on applying denoising filter followed by image sharpening using grid warping.

II. 3D object restoration

In optical microscopy, the problem of 3D object restoration is governed by the following operator equation [2]–[4]

$$I(x,y,z) = O(x,y,z) \otimes H(x,y,z). \tag{1}$$

Here, $I(x,y,z)$ is the registered image, $O(x,y,z)$ is the true object to be found, $H(x,y,z)$ — 3D point spread function (PSF), $\otimes$ — sign of 3D convolution. Generally, there is only finite number N of cross section images for vertical variable $z \in \{z_1,\dots,z_N\}$ available for 3D object reconstruction. Since the vertical resolution of optical microscopy is significantly smaller than the horizontal one we turn from (1) to the following asymmetrical discrete form of (1):

$$I_m(x,y,z) \equiv I(x,y,z_m) = \sum_{n=1}^{N} O(x,y,z_n) * H_{n-m}(x,y). \tag{2}$$

Here, $\{I_m\}$ is the stack of registered images, $\{O_n = O(x,y,z_n)\}$ is the stack of true object cross sections, $H_{n-m}(x,y) = H(x,y,z_n - z_m)\Delta z$, Δz — distance between cross section planes with the indices n and m (n, $m = 1,2,\dots,N$), $*$ is the sign of 2D convolution. Since the problem of direct deconvolution and sectioning of 3D object usually needs intense computations, Fourier transform is applied (2) and the convolution theorem is utilized. As a result, we obtain equations in Fourier images $\widehat{I}_m, \widehat{O}_m, \widehat{H}_m$ of functions I_m, O_m, H_m for each 2D spectral variable (u,v):

$$\widehat{I}_m(u,v) = \sum_{n=1}^{N} \widehat{O}_n(u,v) \cdot \widehat{H}_{n-m}(u,v),\ m = 1,2,\dots,N. \tag{3}$$

Obviously, (3) is a linear system of algebraic equations at each point (u,v) for the found vector $\overrightarrow{O}(u,v) = (\widehat{O}_1(u,v), \widehat{O}_2(u,v), \dots, \widehat{O}_N(u,v))$ and $N \times N$ matrix S of coefficients $\overrightarrow{H}(u,v) = (\widehat{H}_1(u,v), \widehat{H}_2(u,v), \dots, \widehat{H}_N(u,v))$. In operator notations (3) takes the form

$$S\overrightarrow{O} = \overrightarrow{I}. \tag{4}$$

We use iterated Tikhonov regularization method [5] to work with (4) in case of its right part containing distortions mentioned above. The iterations start from $\overrightarrow{O}^0 = (0,0,\dots,0)$ and are updated using the formula

$$\overrightarrow{O}^{k+1} = (E+\mu S^*S)^{-1}\overrightarrow{O}^k + \mu(E+\mu S^*S)^{-1}S^*\overrightarrow{I},\ k = \overline{1,K}. \tag{5}$$

Note that the parameter $\mu > 0$ and the number of iterations K should be chosen according to the trade-off between a rapid initial sectioning with the smallest number of iterations for a rough visualization of layers at relatively large values μ and

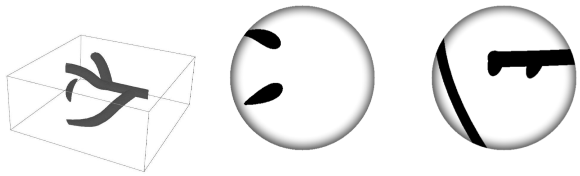

Fig. 1. True 3-D object and its original cross sections with the numbers 3 and 10.

Fig. 2. Distorted images at cross sections 3, 10, and 19.

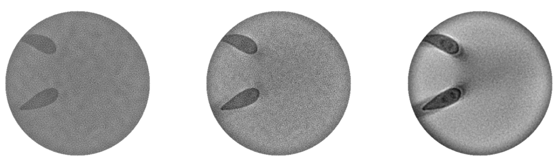

Fig. 3. Sectioning of the layer 3 with the number of iterations $K = 40$ and $\mu = 0.1$, $\mu = 0.01$ and $\mu = 0.001$.

thorough restoration with identifying the fundus texture due to additional iterations applied for small μ [6].

We present results of sectioning for the phantom translucent 3D object of vessels with the number of layers $N = 20$. True 3D object and corresponding original cross-sections are shown in Figure 1. The noise of light-sensitive sensors is modeled by Poisson noise, which has been added to captured images $\{i_m\}$. The typical noise level is about 2% corresponding to 100000 photons per unit intensity of the pixel. The distorted images for the layers with the numbers 3, 10, and 19 are shown in Figure 2. It is easy to see true cross sections distorted with defocused near-depth layers.

Figure 3 shows the typical results of deconvolution with various values of the parameter μ: good sectioning with refining from near-depth layers and residual distortions caused by Poisson noise taken into account. Since Poisson noise is applied at each focal plane cross section independently, we use special methods of three-dimensional post-processing for suppression.

III. Grid warping for image sharpening

A. Introduction

Typical image sharpening algorithms try to improve the high-frequency information of the image. The simplest deblurring algorithm is unsharp mask method that simply amplifies high-frequency information (see Figure 4):

$$I_\alpha = \alpha I + (1-\alpha)(I \otimes G_\sigma),$$

where α is the amplification factor, G_σ is the 3D Gaussian filter, σ is the scale parameter that defines the range of frequencies to be amplified.

Regularization-based methods [7]–[9] use a parameter to set a compromise between smooth result with blurry edges and sharp result with artifacts.

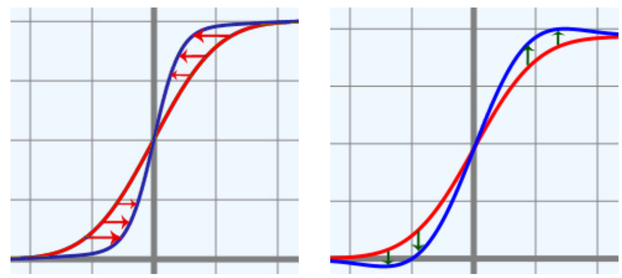

(a) (b)

Fig. 4. The idea of edge sharpening by grid warping: (a) Grid warping: pixels are shifted; (b) Typical deblurring approach: pixel values are modified.

Grid warping algorithms use another approach to make the image sharper: instead of changing pixel values they transform the pixel grid so that the pixels near the edge move towards the edge centerline [10]. It makes the edge sharper, but does not add noise or ringing effect.

The warping approach for image enhancement was introduced in [11]. The warping of the grid is performed according to the solution of a differential equation that is derived from the warping process constraints. The solution of the equation is used to move the edge neighborhood closer to the edge, and the areas between edges are stretched. The method has several parameters, and the choice of optimal values for the best result is not easy. Due to the global nature of the method the resulting shapes of the edges are sometimes distorted.

In [11] the warping map is computed directly using the values of left and right derivatives. In both methods [11] and [12] the pixel shifts are proportional to the gradient values. It results in oversharpening of already sharp and high contrast edges and insufficient sharpening of blurry and low contrast edges. Both methods also introduce small local changes in the direction of edges and produce aliasing effect due to calculation of horizontal and vertical warping components separately.

The work [10] overcomes the drawbacks of the methods [11] and [12]. It constructs the pixel density map that defines the target pixel density after grid warping. The warping vectors are found from a solution of Poisson equation. The work [13] extends the grid warping algorithm for 3D image sharpening and proposes a direct method for finding warping vectors from the density map. Using pure 3D sharpening algorithm instead of sharpening each slice independently increases the quality of corners and planes that lie nearly parallel to the slices.

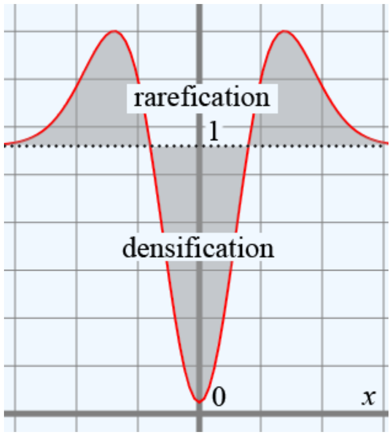

Fig. 5. Example of proximity function for edge sharpening

In this section we present the key moments of the 3D grid warping algorithm.

B. One-dimensional grid warping

We describe the pixel displacement vectors for one-dimensional edge profile centered at $x = 0$ by the proximity function $p(x) : p(x) = 1 + d'(x)$, where $d(x)$ is the displacement function $d(x) : x \to x + d(x)$. The displacement function can be calculated from proximity function using the equation

$$d(x) = \int_{-\infty}^{x} (p(y) - 1)dy. \quad (6)$$

The proximity is the distance between adjacent pixels after image warping. If the proximity function $p(x)$ is less than 1, then the area is densified at the point x (see Fig. 5). If the proximity is greater than 1, then the grid is rarefied. For a non-warped image $p(x) \equiv 1$.

The proximity function greatly influences the result of the edge warping. On the one hand, the edge slope should become steeper. On the other hand, the area near the edge should not be stretched over some predefined limit to avoid wide gaps between adjacent pixels in the discrete case. The necessary conditions for density and proximity functions are stated in [10].

We use the following proximity function constructed as the difference of Gaussian functions

$$p(x) = 1 + \alpha \frac{G_\sigma(x) - G_{k\sigma}(x)}{G_\sigma(0) - G_{k\sigma}(0)}, \quad (7)$$

where $G_\sigma = \frac{1}{\sigma\sqrt{2\pi}} \exp\left(\frac{-x^2}{2\sigma^2}\right)$, α is the strength of warping effect, k is the parameter that controls the area of rarefication. We use $\alpha = 1$, $k = 2$. Parameter σ depends on the blur level of the input image.

C. 3D grid warping

In the three-dimensional case the displacement is a vector field $\vec{d}(x, y, z)$ which is connected to the proximity function by the equation

$$p(x, y, z) = 1 + \operatorname{div} \vec{d}(x, y, z).$$

For known $p(x, y, z)$ the displacement function is obtained from the solution of the equation

$$\vec{d}(x, y, z) = \nabla u(x, y, z),$$
$$\begin{cases} \Delta u & = p(x, y, z) - 1, \\ u(x, y, z) & = 0 \text{ at image borders.} \end{cases}$$

We suggest the following method for calculating the proximity function in the two-dimensional case using one-dimensional proximity function $p(t)$:

$$p(x, y, z) = \frac{\sum_{(x_e, y_e, z_e) \in N(x,y,z)} w(x_e, y_e, z_e) p(x_n)}{\sum_{(x_e, y_e, z_e) \in N(x,y,z)} w(x_e, y_e, z_e)},$$
$$w(x_e, y_e) = G_\sigma(x_t) |\vec{g}(x_e, y_e, z_e)|,$$

where $N(x, y, z)$ is the set of edge points in the neighborhood of (x, y). The values x_n and x_t are projections of the vector $(x - x_e, y - y_e, z - z_e)$ on the edge gradient vector $\vec{g}(x_e, y_e, z_e)$ and on its perpendicular. Edges are detected using Canny edge detection algorithm with zero thresholds [14].

The solution of the equation can be found directly:

$$\vec{d}(x, y, z) = \frac{\sum_{(x_e, y_e, z_e) \in N(x,y,z)} G_\sigma(x_t) d(x_n) \vec{g}(x_e, y_e, z_e)}{\sum_{(x_e, y_e, z_e) \in N(x,y,z)} G_\sigma(x_t) \vec{g}(x_e, y_e, z_e)}.$$

Finally we perform interpolation on the non-regular pixel grid. The work [10] proposes taking all neighboring pixels (x_k, y_k, z_k) of the pixel (x, y, z) and performing weighted averaging

$$I_R(x, y, z) = \frac{\sum_k I(x_k, y_k, z_k) q(x, y, z, x_k, y_k, z_k)}{\sum_k I(x_k, y_k, z_k)},$$

where

$$q(x, y, z, x_k, y_k, z_k) =$$
$$= \exp\left(-\frac{(x - x_k)^2 + (y - y_k)^2 + (z - z_k)^2}{2\sigma_0^2}\right),$$
$$\sigma_0 = 0.3$$

IV. Experiments

We have used the following scheme for the improvement of the 3D object reconstruction result for the phantom translucent 3D object of vessels with the number of layers $N = 20$:

1. Perform the interpolation in z direction to make the resolution isotropic using bicubic interpolation.

2. Apply 3D Gaussian filter with $\sigma = 3$ to suppress the noise and to smooth the effect of mixing the neighboring slices.

3. Perform 3D sharpening using grid warping with $\sigma = 3$ to reduce the blur effect from the Gaussian filter.

4. Return to the original resolution in z direction.

The results of 3D object reconstruction images are shown in Fig. 6 and Fig. 7. The size of the used 3D images is $512 \times$

512×50. Two models are considered: the first model contains large vessels while the second one contains thin vessels. It can be seen that the use of a higher value of Gauss filter parameter results in stronger noise suppression and reducing the effect of mixing the data from neighboring planes. At the same time, very high Gauss filter parameter makes the image too blurred. The experiments have also shown no difference in processing the images obtained using different μ.

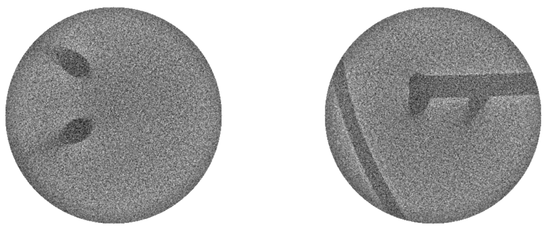

Input images

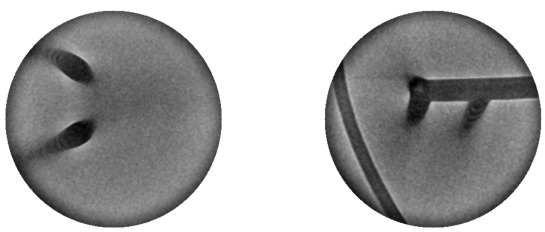

The result of post-processing:
Blur $\sigma = 1.5$, warping $\sigma = 3$

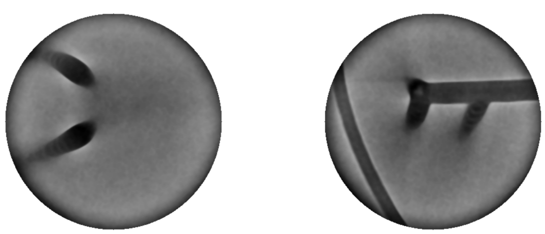

The result of post-processing:
Blur $\sigma = 2.5$, warping $\sigma = 3$

Fig. 6. Results of 3D image enhancement for large vessels model obtained for $\mu = 0.01$

V. Conclusion

Grid warping algorithm has been applied for enhancement of the phantom translucent 3D object images of vessels. The image of vessels had benn processed by Tikhonov regularization method. We found that even small sigma significantly suppresses the noise, and further increase of sigma leads to smoothing the effect of mixing the data from neighboring planes. The suggested method looks promising to be used for fundus images enhancement obtained by different 3D imaging technologies.

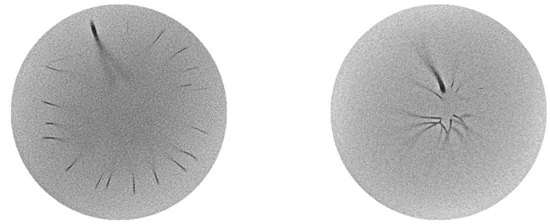

Input images

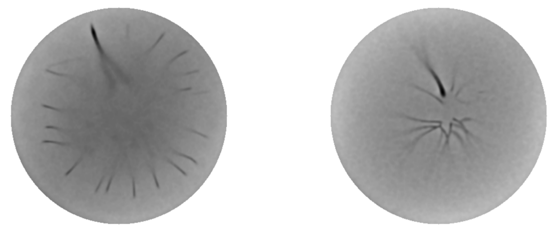

The result of post-processing:
Blur $\sigma = 2.5$, warping $\sigma = 3$

Fig. 7. Results of 3D image enhancement for thin vessels model obtained for $\mu = 0.01$

Acknowledgment

The work was supported by Russian Foundation for Basic Research grant 15-29-03896.

References

[1] A.V. Larichev, P.V. Ivanov, N.G. Iroshnikov, V.I. Shmalhauzen, L.J. Otten, "Adaptive system for eye-fundus imaging," *Quantum Electronics*, vol. 32, pp. 902–908, 2002.

[2] D. Agard, "Optical sectioning microscopy: cellular architecture in three dimensions," *Ann. Rev. Biophys. Bioeng*, vol. 13, pp. 191–219, 1984.

[3] K. Castleman, *Digital Image Processing*. Pearson Education, 2007.

[4] Q. Wu, F. Merchant, K. Castleman, *Microscope image processing*. Academic Press, 2008.

[5] A.B. Bakushinsky, A.V. Goncharsky, *Iterative methods for solving ill-posed problems (In Russian)*. Nauka, 1989.

[6] A.V. Razgulin, N.G. Iroshnikov, A.V. Larichev, S.D. Pavlov, T.E. Romanenko, "On a problem of numerical sectioning in ophtalmology," *Computer Optics*, vol. 39, no. 5, pp. 777–786, 2015 (in Russian).

[7] M. Almeida and M. Figueiredo, "Parameter estimation for blind and non-blind deblurring using residual whiteness measures," *IEEE Transactions on Image Processing*, vol. 22, pp. 2751–2763, 2013.

[8] J. Oliveira, J. M. Bioucas-Dia, and M. Figueiredo, "Adaptive total variation image deblurring: A majorization-minimization approach," *Signal Processing*, vol. 89, pp. 1683–1693, 2009.

[9] S. D. Babacan, R. Molina, and A. K. Katsaggelos, "Variational bayesian blind deconvolution using a total variation prior," *IEEE Transactions on Image Processing*, vol. 18, pp. 12–26, 2009.

[10] A. Nasonova and A. Krylov, "Deblurred images post-processing by poisson warping," *IEEE Signal Processing Letters*, vol. 22, no. 4, pp. 417–420, 2015.

[11] N. Arad and C. Gotsman, "Enhancement by image-dependent warping," *IEEE Transactions on Image Processing*, vol. 8, pp. 1063–1074, 1999.

[12] J. Prades-Nebot et al., "Image enhancement using warping technique," *IEEE Electronics Letters*, vol. 39, pp. 32–33, 2003.

[13] A. S. Krylov and A. V. Nasonov, "3d image sharpening by grid warping," *Lecture Notes in Computer Science (IScIDE2015)*, vol. 9242, pp. 441–450, 2015.

[14] J. Canny, "A computational approach to edge detection," *IEEE Trans. Pattern Analysis and Machine Intelligence*, vol. 8, pp. 679–698, 1986.